2017 IEEE International Conference on Robotics and Automation (ICRA)
Singapore, May 29 - June 3, 2017

Balancing Control of a Robot Bicycle with Uncertain Center of Gravity*

Chun-Feng Huang, Yen-Chun Tung, and Ting-Jen Yeh[1]

Abstract— **In this research, a small humanoid robot and a bicycle of comparable size are constructed. Like the human rider, the robot is designed to pedal, balance and steer the bicycle. We particularly focus on the design of control system for the robot to balance and steer the bicycle using the handlebar. The control system is novel that it is capable of estimating the uncertain center of gravity of the robot-bicycle system and then incorporating such an estimation to enhance control performance. The control system design is based on a general control framework which can establish asymptotic stability under unknown measurement biases. The stability of the control system is theoretically proved and a systematic procedure to compute the control parameters is given. Both simulations and experiments verify that the proposed controller can automatically counteract the mass imbalance in the system and allow the robot to perform straight-line steering.**

I. INTRODUCTION

As the first kind of personal mobility vehicles ever invented, bicycles play an important role in the history of transport. Bicycles are light-weight and are solely propelled by human power. They can contribute to the reduction of traffic congestion and air pollution in urban areas. Bicycles are classified as single-track vehicles and display interesting dynamic behaviour. For instance, they are statically unstable in the lateral direction which requires manual control to balance the vehicle, but over certain speeds, bicycles can automatically develop lateral stability without human intervention. The intriguing behaviour of bicycles poses challenge problems in modeling and control which has attracted attention from automatic control research community. For instance, the authors in [1] designed a feedback-linearization controller on a nonlinear, two DOF bicycle model which uses longitudinal acceleration, rider's leaning torque, and steering angle as the control inputs. The simulated control system performance is compared to the experimental behavior of a human rider actually riding a bicycle.

Recently, advances in digital computers, sensor and actuator technologies have raised research interests in developing self-balancing robot bicycles. A self-balancing bicycle uses inertia sensors to detect the posture (mainly the roll angle) of the bicycle and actuators to bring it to balance. There exist several mechatronic solutions to construct a self-balancing bicycle. For example, in [2], using the steering angle as the input, a PD control is designed to stabilize the roll motion of the bicycle. Similar PD type control was also used in [3] except that the movement of an inverted pendulum which simulates the COG motion of the rider is treated as an extra control input. A gyroscopic stabilization unit, which consists of two coupled gyroscopes spinning in opposite directions, was adopted in Beznos et al.[4] to balance a bicycle. The authors therein controlled the precession of the gyroscopes to generate a gyroscopic torque to counteract the destabilizing gravitational torque. Lee and Ham[5] proposed a load mass system to balance the bicycle. The control strategy was developed to turn the bicycle system left or right by moving the center of a load mass accordingly. A well-known self-balancing robot bicycle, Murata Boy, was developed by Murata in 2005 [6]. Murata Boy contains a reaction wheel whose speed change generates a reaction torque to balance the bicycle.

In this research, a small humanoid robot and a bicycle of comparable size are constructed as shown in Fig.1. Like the human rider, the robot is designed to pedal, balance and steer the bicycle. We particularly focus on the design of control system for the robot to balance and steer the bicycle using the handlebar. The control system is novel that it is capable of estimating the uncertain center of gravity of the robot-bicycle system and then incorporating such an estimation to enhance control performance. The control system design is based on a general control framework which can establish asymptotic stability under unknown measurement biases. The paper is organized as follows: A model that describes the lateral dynamics of a bicycle is given in Section II. Section III shows how the dynamic model can be converted into a form tractable by the control framework so as to design the balancing control system. The performance of the control system is verified numerically in Section IV. Section V describes the hardware setup of the bicycle robot system and performs experimental validation on the control performance. Finally, conclusions are given in Section VI.

II. MODELING OF THE LATERAL DYNAMICS

In this section, a model that describes the lateral dynamics of a bicycle is derived. The modeling here follows a similar approach adopted in [7] and [2]. It starts with analyzing the kinematic relations among crucial motion variables.

A. Kinematic Analysis

Fig. 2 shows the top view of a bicycle in which O_g is the center of gravity (COG) of the bicycle, O_r is the center of the rear wheel, O_f is the center of the front wheel. Assume the rear wheel is pedaled with speed v_0 and the front wheel is steered so that a directional angle η is resulted. Pedaling and steering actions make the bicycle turn with respect to

*This work is sponsored by Ministry of Science and Technology in Taiwan.

[1]All authors are with the Department of Power Mechanical Engineering, National Tsing Hua University, Hsinchu 30013, Taiwan benson516@hotmail.com; yctung1992@gmail.com; tyeh@pme.nthu.edu.tw

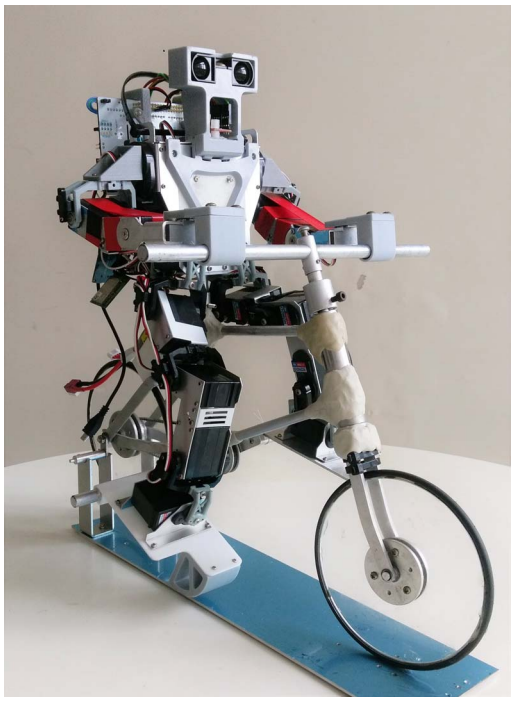

Fig. 1. Photo of the robot-bicycle system

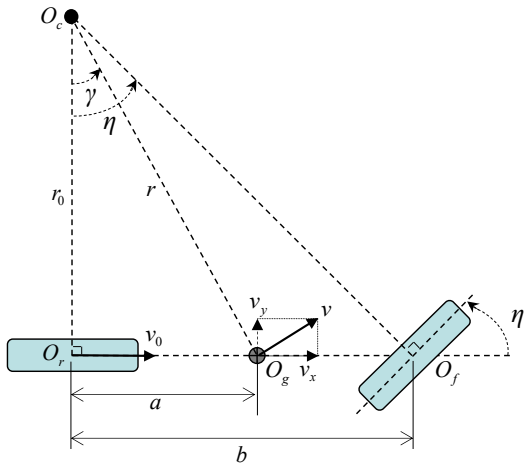

Fig. 2. Top view of a bicycle

an instantaneous center of rotation O_c, which under the no-slip condition, is the intersection of the two extension lines respectively from the axles of the front and rear wheels. Denoting $a = \overline{O_rO_g}$, $b = \overline{O_rO_f}$, $r_0 = \overline{O_cO_r}$, $r = \overline{O_cO_g}$, and $\gamma = \angle O_rO_cO_g$, the following geometric relations hold:

$$r = \frac{a}{\sin\gamma}, \tag{1}$$

and

$$r_0 = \frac{a}{\tan\gamma} = \frac{b}{\tan\eta}. \tag{2}$$

The ratio $\frac{v_0}{r_0}$ is equal to the yaw rate of the bicycle and is denoted by $\dot{\phi}$. Using the second equality in (2), $\dot{\phi}$ can be written as

$$\dot{\phi} = \frac{\tan\eta}{b} v_0. \tag{3}$$

Let v be the magnitude of the bicycle's velocity at the COG O_g, and v_x and v_y be the components of the velocity along and perpendicular to the bicycle body. While the rigidity of the bicycle body makes v_x equal to v_0, v and v_y are related to v_0 respectively by

$$v = r\dot{\phi} = \frac{a\tan\eta}{b\sin\gamma} v_0, \tag{4}$$

and

$$v_y = v\sin\gamma = \frac{a\tan\eta}{b} v_0. \tag{5}$$

B. Dynamic Analysis

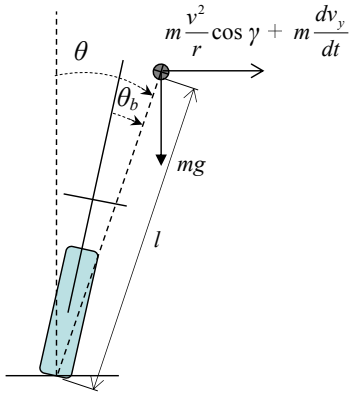

Fig. 3. Frontal view of a bicycle

In the the frontal view shown in Fig. 3, the bicycle plus the robot is modeled as an inverted pendulum whose mass m is concentrated at the COG. The COG is located at a distance of l from the ground contact point with a roll angle θ. We also consider that because of mass imbalance, the COG is not exactly on the center line of the bicycle but is offseted by an angle θ_b. Notice that the inverted pendulum system in Fig.3 may not be in an inertia frame when the bicycle is in motion. Therefore, in addition the gravitational force, one also has to consider the inertia force $m\frac{dv_y}{dt}$ and the centrifugal force $m\frac{v^2}{r}\cos\gamma$ acting on COG when deriving the dynamic equation. Applying Newton's law and substituting the expressions of v and v_y in (4) and (5), the lateral dynamics is derived as:

$$\begin{aligned} m\ell^2\ddot{\theta} &= m\ell\cos\theta\left(\frac{v^2}{r}\cos\gamma + \frac{dv_y}{dt}\right) + mg\ell\sin\theta \\ &= m\left(\frac{v_0^2}{b}\tan\eta + \frac{av_0\sec^2\eta}{b}\dot{\eta}\right) + mg\ell\sin\theta \end{aligned} \tag{6}$$

in which the second equality also utilizes the relation $\tan\gamma = \frac{a}{b}\tan\eta$ inferred from (2).

When both the the directional angle η and the roll angle θ are small, the nonlinear dynamics in (6) can be further linearized as

$$m\ell^2\ddot{\theta} \approx m\left(\frac{v_0^2}{b}\eta + \frac{av_0}{b}\dot{\eta}\right) + mg\ell\theta \tag{7}$$

It should be noted that the directional change of the front wheel is due to the vertical projection of the rotation of the steering handlebar via the caster angle of the front fork assembly[2]. Denoting the steering angle of the handlebar by δ and the caster angle by ε_0, the directional angle η can be expressed as

$$\eta = \sin\varepsilon_0 \cdot \delta. \tag{8}$$

Substituting the above expression into (7) yields

$$m\ell^2\ddot{\theta} = m\frac{av_0\sin\varepsilon_0}{b}(\frac{v_0}{a}\delta + \dot{\delta}) + mg\ell\theta \tag{9}$$

III. BALANCING CONTROL OF THE BICYCLE

According to (9), the open-loop transfer function from δ to θ can be derived as

$$\frac{\theta(s)}{\delta(s)} = \frac{\frac{a\sin\varepsilon_0 v_0}{b\ell^2}(s+\frac{v_0}{a})}{s^2 - \frac{g}{\ell}} \tag{10}$$

The system is unstable due to the inverted pendulum mode which contains an unstable pole at $\sqrt{\frac{g}{\ell}}$. As a result, feedback control is needed to modulate the steering angle to stabilize/balance the bicycle. Typically the balancing control system for wheeled inverted pendulum (WIP) vehicles like bicycles relies on measurements from the inertia measurement unit (IMU) installed on the vehicle body. The signals of the IMU are fusioned to compute the absolute orientation of the IMU's sensor frame. In the current study, the IMU is installed on the plane of symmetry of the bicycle body as the other WIP vehicles. Because of possible uncertain mass imbalance, there could exist an uncertain offset between the roll angle computed by the IMU and that of the COG. Such an uncertain offset is denoted as θ_b in Fig. 3; thus the computed roll angle for feedback is $\theta - \theta_b$ instead of θ. Equivalently, θ_b can be viewed as a measurement bias to the COG angle θ.

The challenge task in the control system design is to achieve asymptotic stability for the roll angle θ under the uncertain measurement bias θ_b. If asymptotic stability can not be achieved, say a constant steady-state error exists in θ, by conducting steady-state analysis on (9), one can find that a non-zero steering angle δ is resulted, which in turn leads to a non-zero yaw rate ($\dot{\phi}$) according to the kinematic relations in (8) and (3). A non-zero yaw rate would cause the bicycle robot to circle around and hinder it from following a straight path.

In the authors' previous work on balancing control of a pedaled unicycle[8], a control framework which can achieve asymptotic stability in the presence of measurement bias was proposed. Such a control framework can be used to resolve the control problem encountered in the bicycle case. To convert the model of lateral dynamics into a state-space form tractable by the control framework, we define the state vector $\mathbf{x}$ as $\begin{bmatrix} \theta & \dot{\theta} & \delta \end{bmatrix}^T$ and redefine a new control input as

$$\mathbf{u} = \dot{\delta} + \frac{v_0}{a}\delta. \tag{11}$$

The linearized lateral dynamics of the bicycle is written in the state-space form as

$$\dot{\mathbf{x}} = \mathbf{A}\mathbf{x} + \mathbf{B}\mathbf{u}, \tag{12}$$

where $\mathbf{A} = \begin{bmatrix} 0 & 1 & 0 \\ \frac{g}{\ell} & 0 & 0 \\ 0 & 0 & -\frac{v_0}{a} \end{bmatrix}$, $\mathbf{B} = \begin{bmatrix} 0 \\ \frac{a\sin\varepsilon_0 v_0}{b\ell^2} \\ 1 \end{bmatrix}$. As for the output equation, other than the roll angle $\theta - \theta_b$, steering angle δ is measurable, and sensor fusion algorithm also generates the roll rate $\dot{\theta} - \dot{\theta}_b$ which equals $\dot{\theta}$ because θ_b is a constant. Thus the output vector $\mathbf{y}$ is given by

$$\mathbf{y} = \mathbf{x} + \mathbf{C}\varphi \tag{13}$$

where $\mathbf{C} = \begin{bmatrix} -1 & 0 & 0 \end{bmatrix}^T$ and $\varphi = \theta_b$.

Given the state equation (12) and the output equation (13), the control objective in this research is to use the feedback from $\mathbf{y}$ to devise a control law for $\mathbf{u}$ that can make $\mathbf{x}$ asymptotically converge to a reference state $\mathbf{x}_d$. The major challenge here is that the output is contaminated by an unknown output bias θ_b, so an adaptive scheme would be helpful for on-line estimating and then canceling θ_b form $\mathbf{y}$. While the general setting of the control problem with $\mathbf{x} \in R^n$, $\mathbf{u} \in R^p$, and $\varphi \in R^q$ (which correspond to $\mathbf{A} \in R^{n\times n}$, $\mathbf{B} \in R^{n\times p}$, and $\mathbf{C} \in R^{n\times q}$) was studied in [8], the work therein leads to a control system which can achieve asymptotic state regulation under uncertain measurement bias. Details about the control system are described in the following proposition.

Proposition 3.1: Given the state equation and the output equation in (12) and (13), the control law takes the form of

$$\mathbf{u} = -\mathbf{K}(\hat{\mathbf{x}} - \mathbf{x}_d) + \mathbf{u}_d \tag{14}$$

with an estimation law

$$\dot{\hat{\varphi}} = \mathbf{K}_\varphi(\hat{\mathbf{x}} - \mathbf{x}_d). \tag{15}$$

In (14) and (15), $\hat{\varphi}$ is the estimation for the uncertain measurement bias φ, $\hat{\mathbf{x}}$ is the estimated state vector and is computed by $\mathbf{y} - \mathbf{C}\hat{\varphi}$, $\mathbf{x}_d$ is a constant reference command and $\mathbf{u}_d$ is the corresponding feed-forward control and both of which should satisfy the constraint of equilibrium

$$\mathbf{A}\mathbf{x}_d + \mathbf{B}\mathbf{u}_d = 0 \tag{16}$$

The feedback gain matrix $\mathbf{K}$ should be chosen to make $\mathbf{A}_c = \mathbf{A} - \mathbf{B}\mathbf{K}$ a stable matrix, and the estimation gain matrix $\mathbf{K}_\varphi$ is computed via the following three-step procedure:

1) Choose $\mathbf{Q}_1 = \mathbf{Q}_1^T > 0$, $\mathbf{Q}_2 = \mathbf{Q}_2^T > 0$. Compute the solution $\mathbf{R} = \mathbf{R}^T > 0$ to the Lyapunov matrix equation

$$\mathbf{R}\mathbf{A}_\mathbf{c} + \mathbf{A}_c^T\mathbf{R} = -\mathbf{Q}_1 < 0 \tag{17}$$

and then the matrix

$$\mathbf{S} = (\mathbf{Q}_2\mathbf{A}^{-1})^T + \mathbf{R}\mathbf{B}\mathbf{K}. \tag{18}$$

2) Define

$$\mathbf{D} = \mathbf{I}_{n\times n} - \mathbf{S}\mathbf{C}(\mathbf{C}^T\mathbf{A}^T\mathbf{S}\mathbf{C})^{-1}\mathbf{C}^T\mathbf{A}^T \tag{19}$$

$$\mathbf{W} = \mathbf{C}(\mathbf{C}^T\mathbf{A}^T\mathbf{S}\mathbf{C})^{-1}\mathbf{C}^T\mathbf{A}^T \tag{20}$$

and choose $\mathbf{Q}_3 = \mathbf{Q}_3^T > 0$. Compute $\mathbf{P}$, the solution to the following Riccati equation:

$$\mathbf{A}_c^T \left(\mathbf{D}^T + \mathbf{W}^T\mathbf{Q}_2\mathbf{A}^{-1}\right)^T \mathbf{P} + \mathbf{P}\left(\mathbf{D}^T + \mathbf{W}^T\mathbf{Q}_2\mathbf{A}^{-1}\right)\mathbf{A}_c + \mathbf{P}\left(\mathbf{W} + \mathbf{W}^T\right)\mathbf{P} = -\mathbf{Q}_3 < 0. \tag{21}$$

3) $\mathbf{K}_\varphi$ is computed by

$$\mathbf{K}_\varphi = (\mathbf{C}^T\mathbf{A}^T\mathbf{S}\mathbf{C})^{-1}\mathbf{C}^T\mathbf{A}^T\mathbf{P} \in \mathbb{R}^{q\times n} \tag{22}$$

The stability of the closed-loop system is guaranteed by the following theorem.

Theorem 3.1: The closed-loop system (12), (13), (14), and (15) is asymptotically stable that $\mathbf{x} \to \mathbf{x}_d$ and $\hat{\varphi} \to \varphi$ as $t \to \infty$ if $\mathbf{A}$ is invertible, $(\mathbf{A}, \mathbf{B})$ is controllable, and $\mathbf{C}$ is full rank.

The sketch of the proof for the theorem is given below:

Proof: Consider the function

$$V = (\hat{\mathbf{x}} - \mathbf{x}_d)^T\mathbf{P}(\hat{\mathbf{x}} - \mathbf{x_d}) + \tilde{\varphi}^T\mathbf{C}^T\mathbf{Q}_2\mathbf{C}\tilde{\varphi} + \dot{\tilde{\mathbf{x}}}^T\mathbf{R}\tilde{\mathbf{x}}, \tag{23}$$

where $\tilde{\varphi} = \hat{\varphi} - \varphi$ is the estimation error and $\tilde{\mathbf{x}} = \mathbf{x} - \mathbf{x}_d$ is the state error. It should be noted that $\mathbf{C}$ is full rank and $\mathbf{Q}_2 > 0$, so we have $\mathbf{C}^T\mathbf{Q}_2\mathbf{C} > \mathbf{0}$. This, together with $\mathbf{P}$, $\mathbf{R} > \mathbf{0}$, makes $V \geq 0$. Furthermore, $V = 0$ if and only if $\hat{\mathbf{x}} = \mathbf{x}_d$,$\tilde{\varphi} = \mathbf{0}$, and $\dot{\tilde{\mathbf{x}}} = \mathbf{0}$. Because $\hat{\mathbf{x}} = \mathbf{x}_d$, $\tilde{\varphi} = \mathbf{0}$ means $\tilde{\mathbf{x}} = \mathbf{0}$, and by substituting the control law (14) to the state equation (7) and utilizing the structural constraint (16) we have

$$\dot{\tilde{\mathbf{x}}} = \mathbf{A}_c\tilde{\mathbf{x}} + \mathbf{B}\mathbf{K}\mathbf{C}\tilde{\varphi}, \tag{24}$$

the necessary and sufficient condition for $V = 0$ is equivalent to $\tilde{\mathbf{x}} = 0$, and $\tilde{\varphi} = \mathbf{0}$. The function V is thus positive-definite in the space of $\begin{bmatrix} \tilde{\mathbf{x}} & \tilde{\varphi} \end{bmatrix}^T$ and can be viewed as a Lyapunov function candidate. With $\mathbf{K}$ and $\mathbf{K}_\varphi$ designed by the procedure stated in the theorem, it can be shown in [8] that $\dot{V}$ is negative definite which leads $\tilde{\mathbf{x}} \to \mathbf{0}$, and $\tilde{\varphi} \to \mathbf{0}$. ■

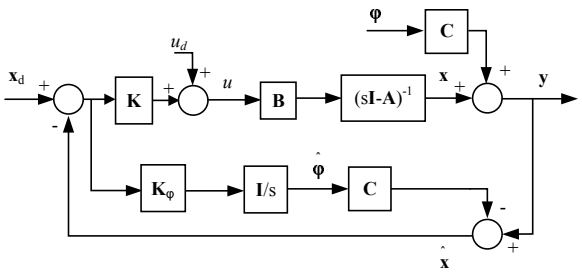

Fig. 4. Block diagram of the proposed control structure

IV. SIMULATION STUDIES

Although the proposed balancing controller is designed based on the linearized model, for numerical verifications, it is applied to the nonlinear model in (6) to simulate the control performance. The system parameters used are listed in Table I.

The control gain $\mathbf{K}$, which is designed using LQR method, is given by $\mathbf{K} = \begin{bmatrix} 73.6074 & 12.178 & 0 \end{bmatrix}$. Following the design procedure depicted in Section III, the estimator gain matrix is given by $\mathbf{K}_\varphi = \begin{bmatrix} 1.977 & 0.58 & -0.14 \end{bmatrix}$. The corresponding closed-loop poles are -8.8546, $-2.7412 \pm 4.3120i$, and -3.6902 rad/s.

TABLE I

PARAMETERS OF THE BICYCLE MODEL USED IN THE SIMULATIONS

a	0.13 m	m	2.465 kg
b	0.322 m	ℓ	0.2 m
v_0	1.0174 m/s	ε_0	60°

The simulations assume that θ_b is 3°. The performance of the proposed controller is compared to a PD controller in which $u = -\mathbf{K}\mathbf{y}$ that the biased roll angle and the roll rate are directly used for feedback. In the first simulation $\mathbf{x}(0) = \begin{bmatrix} 5° & 10\ °/s & 0° \end{bmatrix}^T$. It is desired to maintain $\mathbf{x} = \mathbf{0}$ (by letting $\mathbf{x}_d = \mathbf{0}$) under the measurement bias θ_b.

Fig. 5 displays the responses of θ, $\dot{\theta}$, and δ for both controllers. From Fig.5, we can see that both controllers stabilize the bicycle. However, the PD controller exhibits steady-state errors in $\theta(\approx -5.994°)$ and $\delta(\approx 21.2°)$ which leads to a steady-state yaw rate as shown in Fig.6. On the other hand, the integral action allows the proposed controller to reject the output bias so that the state errors all settle to zero within 1sec. Fig.5(d) shows that the estimated bias eventually converges to 3°.

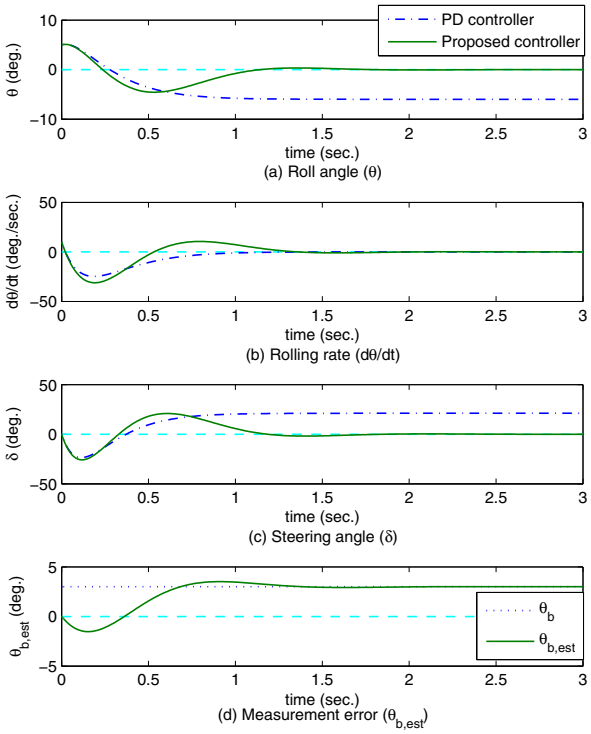

Fig. 5. Simulated state responses for PD controller and the proposed controller

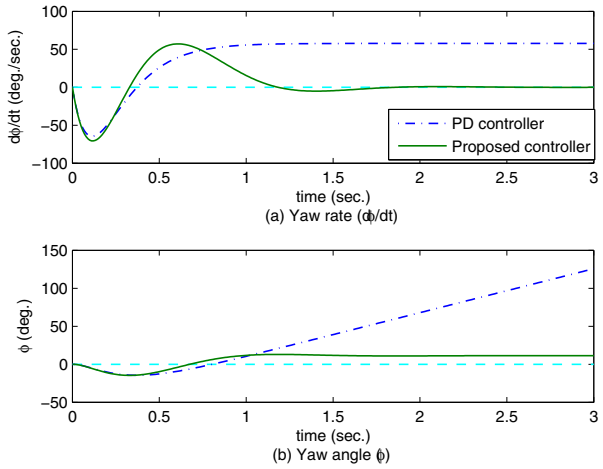

Fig. 6. The yaw rate $\dot{\phi}$ and yaw angle ϕ for PD controller and the proposed controller

V. EXPERIMENTAL VERIFICATIONS

As shown in Fig.7, the constructed humanoid robot has four degrees of freedom in each arm and five degrees of freedom in each leg. The joint angles of the arms and legs are computed by inverse kinematics to achieve the commanded steering angle and pedaling speed. An IMU which contains a three-axis accelerometer and a three-axis gyros is installed on the robot. The sensor fusion algorithm developed previously by the authors[9], which not only considers the multi-axis coupling among the sensor signals but also accounts for the dynamic effects including the longitudinal acceleration and centrifugal acceleration, is adopted to compute the roll angle, roll rate and the yaw rate of the bicycle. Both the sensor fusion and the control algorithm are implemented on STM32F401RE MCU board.

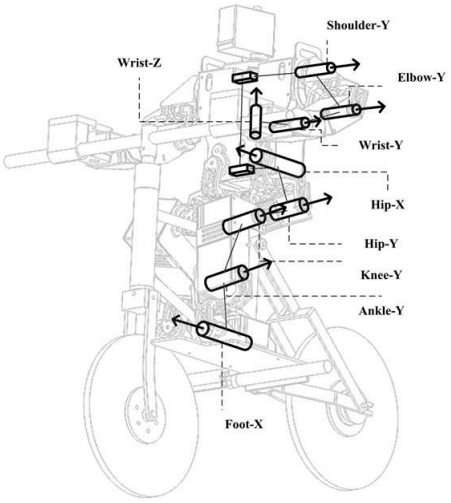

Fig. 7. Schematics of the humanoid robot and the bicycle

Experiments are conducted to verify the balancing performance of the proposed controller. To more clearly examine the impact of measurement bias on the control performance, a $50g$ weight is attached to the right side of the handlebar to make a significant shift on the COG. Both the proposed controller and the PD controller with the same control parameters as those used in simulations are implemented. The responses in Fig.8 indicate that the PD controller is unable to reject the mass imbalance for the steering angle oscillates around -4° persistently. The biased steering angle causes undesirable turning which eventually leads to bicycle fall. Fig.9 shows the responses of the proposed controller. The controller is able to estimate the measurement bias in which the estimation converges to -2.2° at steady state. The steering angle exhibits small oscillation around 0° and the yaw rate converges to zero as well.

Video demonstrations of the balancing experiments can be found in the supplementary video file. Also shown in the video is starting and stopping the bicycle using the proposed balancing controller. However, in this case the control gains require some experimental tuning to accommodate the transient behavior. We also thicken the toe of the robot to make it act as the third support (in addition to two wheels) to maintain bicycle's stability at standstill.

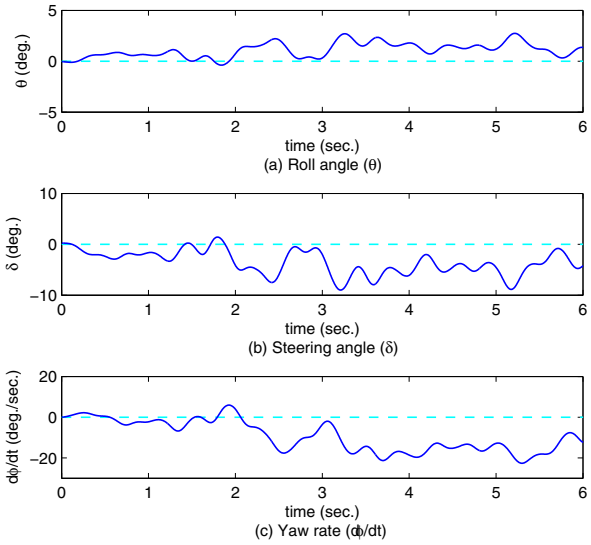

Fig. 8. Experiment responses of the robot-bicycle under PD control

VI. CONCLUSIONS

This paper is devoted to the balancing control of a bicycle via a humanoid robot. The proposed controller is based on the state-space model of the linearized lateral dynamics, and its design is under a general control framework which can achieve asymptotic control performance in the presence of measurement biases. The stability of the control system is theoretically proved and a systematic procedure to compute the control parameters is given. Both simulations and experiments verify that the proposed controller can automatically counteract the mass imbalance in the system and allow the

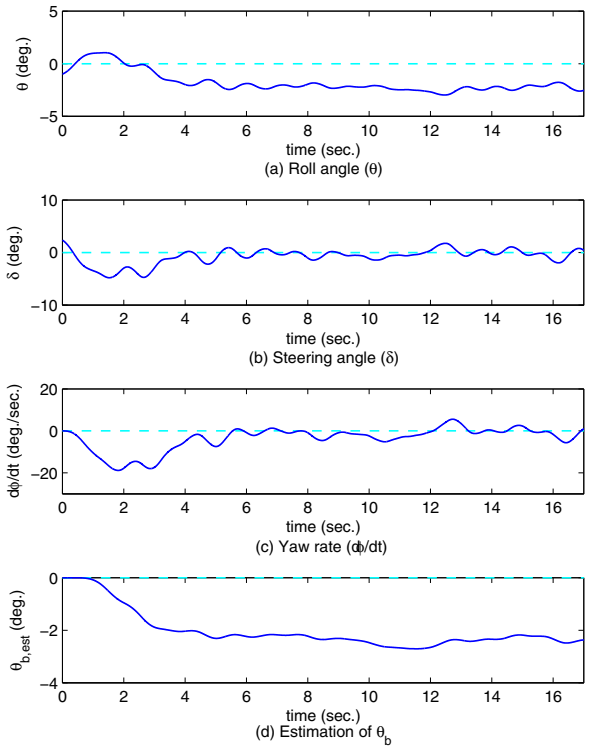

Fig. 9. Experiment responses of the robot-bicycle under the proposed controller

robot to perform straight-line steering. On-going research efforts include incorporating cameras, infrared sensors and so on to study collision avoidance and autonomous navigation of the robot-bicycle system.

ACKNOWLEDGMENT

The authors gratefully acknowledge the support provided by Ministry of Science and Technology in Taiwan.

REFERENCES

[1] P. Wang and J. Yi, "Balance equilibrium manifold and control of rider-bikebot systems," in *American Control Conference (ACC), 2016*. IEEE, 2016, pp. 2168–2174.

[2] Y. Tanaka and T. Murakami, "Self sustaining bicycle robot with steering controller," in *Advanced Motion Control, 2004. AMC '04. The 8th IEEE International Workshop on*, March 2004, pp. 193–197.

[3] K. Iuchi, H. Niki, and T. Murakami, "Attitude control of bicycle motion by steering angle and variable cog control," in *31st Annual Conference of IEEE Industrial Electronics Society, 2005. IECON 2005.*, Nov 2005, pp. 6 pp.–.

[4] A. V. Beznos, A. M. Formal'sky, E. V. Gurfinkel, D. N. Jicharev, A. V. Lensky, K. V. Savitsky, and L. S. Tchesalin, "Control of autonomous motion of two-wheel bicycle with gyroscopic stabilisation," in *Robotics and Automation, 1998. Proceedings. 1998 IEEE International Conference on*, vol. 3, May 1998, pp. 2670–2675 vol.3.

[5] S. Lee and W. Ham, "Self stabilizing strategy in tracking control of unmanned electric bicycle with mass balance," in *Intelligent Robots and Systems, 2002. IEEE/RSJ International Conference on*, vol. 3, 2002, pp. 2200–2205 vol.3.

[6] Murata, "Murata boy." [Online]. Available: http://www.murata.com/

[7] K. J. Astrom, R. E. Klein, and A. Lennartsson, "Bicycle dynamics and control: adapted bicycles for education and research," *IEEE Control Systems*, vol. 25, no. 4, pp. 26–47, Aug 2005.

[8] C.-F. Huang and T. J. Yeh, "Control of a pedaled, self-balanced unicycle with adaptation capability," in *Informatics in Control, Automation and Robotics (ICINCO), 2014 11th International Conference on*, vol. 02, Sept 2014, pp. 120–126.

[9] C. F. Huang, B. H. Dai, and T. J. Yeh, "Observer-based sensor fusion for power-assist electric bicycles," in *2016 American Control Conference (ACC)*, July 2016, pp. 5486–5491.